

# Chitosan-Mediated Synthesis of Gold Nanoparticles on Patterned Poly(dimethylsiloxane) Surfaces

Bo Wang,<sup>†</sup> Ke Chen,<sup>‡</sup> Shan Jiang,<sup>§</sup> François Reincke,<sup>||</sup> Weijun Tong,<sup>†,||</sup> Dayang Wang,<sup>||</sup> and Changyou Gao<sup>\*,†</sup>

*Department of Polymer Science and Engineering, Zhejiang University, Hangzhou 310027, P. R. China, Department of Radio Engineering, Southeast University, Nanjing, P. R. China, Department of Materials Science and Engineering, University of Illinois, Urbana, Illinois 61801, and Max Planck Institute of Colloids and Interfaces, D-14424 Potsdam, Germany*

*Received January 12, 2006; Revised Manuscript Received February 6, 2006*

Synthesis of gold nanoparticles on surfaces has been accomplished by the incubation of poly(dimethylsiloxane) (PDMS) films in tetrachloroauric(III) acid and chitosan solution at room temperature and 4 °C. One important point in the present study is that the synthesis selectively occurred on the PDMS surface. These observations are substantially different from the reaction in solution, in which no particles can be formed at room temperature. Computation of surface plasmon bands (SPBs) based on Mie theory suggests that the particles are partially coated by chitosan molecules, and the experimental results confirm the theoretical calculations. The proposed mechanism is that chitosan molecules adsorbed or printed on the PDMS surfaces act as reducing/stabilizing agents. Furthermore, PDMS films patterned with chitosan could induce localized synthesis of gold nanoparticles in regions capped with chitosan only. In this way, colloidal patterns were fabricated on the surfaces with high spatial selectivity simultaneously with the synthesis of the particles. Surface-induced fluorescence quenching was observed in the regions capped with gold nanoparticles as well.

## Introduction

Metallic nanostructures play a substantial role in nanotechnology. Tremendous efforts have been devoted toward developing new methods of preparing metal nanoparticles with different topologies, such as spheres, wires, and tetrapods.<sup>1</sup> With their interesting chemical and physical properties, gold nanoparticles are ubiquitously used in fundamental and technical fields, such as catalysis, biological labeling, and sensing.<sup>2</sup> In addition, gold nanoparticles can be applied as fluorescence quenchers to monitor receptor/ligand binding and release events through changes in the fluorescence intensity or lifetime, which is of importance for use in fluorescence immunoassays.<sup>2d</sup>

A number of methods have been reported to synthesize gold nanoparticles in both organic and aqueous media.<sup>3</sup> Electropositive gold ions can be reduced by various reagents such as borohydride, amines, alcohols, and carboxylic acids.<sup>1,4</sup> To prevent nanoparticles from aggregating during their synthesis, small organic molecules or polymers must be added to the synthesis medium as stabilizers.<sup>5</sup> Citrate is the most commonly used reducing and stabilizing agent.<sup>6</sup> Polymers are also used to control the rate of the reduction process and thus modulate the shapes and sizes of the resultant particles.<sup>7</sup> Small bioactive molecules and biomacromolecules have been used to synthesize “green” nanoparticles.<sup>8</sup> Metal ions also can be reduced in an intracellular space to form nanoparticles with good monodispersity.<sup>9</sup>

Patterning of metallic structures has a wide spectrum of potential applications in micro-optics and micro-electronics. The

common strategy is assembly of the prepared nanoparticles on patterned surfaces. However, there are many restrictions on the types of substrates and solvents employed. In our opinion, directly localized synthesis of metal nanoparticles can be a solution to this problem.

In this article, we present the chitosan-mediated synthesis of gold nanoparticles on poly(dimethylsiloxane) (PDMS) surfaces under mild conditions. Chitosan is the ( $\beta$ -1,4)-linked glucosamine derivative of the polysaccharide chitin and a biodegradable and biocompatible biopolymer (Figure 1). Payne and co-workers have reported that aminopolysaccharide chitosan can mediate the electrodeposition of nanoparticles for the preparation of patterned devices.<sup>10</sup> Furthermore, chitosan has been adopted as a stabilizer<sup>11</sup> and, more recently, as a reducing agent<sup>12</sup> to synthesize gold nanoparticles in solution as well as in thin films.<sup>13</sup> The size and stability of the prepared nanoparticles depend on the concentration of chitosan.<sup>14</sup> The interaction between chitosan and anionic tetrachloroauric ions involves the electrostatic attraction between metal anions and protonated amine groups.<sup>15</sup> Prepared gold nanoparticles are expected to be biocompatible. In the current work, we demonstrate a direct method for synthesizing gold nanoparticles selectively on polymer surfaces under mild conditions. By selectively adsorbing chitosan or printing chitosan molecules on patterned polymeric surfaces, the patterning of gold nanoparticles was also achieved. Moreover, localized surface-induced fluorescence quenching and surface-enhanced Raman scattering were also observed for the resulting patterned surfaces. The intensity of the fluorescence and Raman bands provides information on the positions of the molecules and cells on the patterned substrates, offering great promise in applications involving sensing of the movement of a single cell or diffusion of a single molecule.

\* To whom correspondence should be addressed. Fax: +86-571-87951948. E-mail: cygao@mail.hz.zj.cn.

<sup>†</sup> Zhejiang University.

<sup>‡</sup> Southeast University.

<sup>§</sup> University of Illinois.

<sup>||</sup> Max Planck Institute of Colloids and Interfaces.

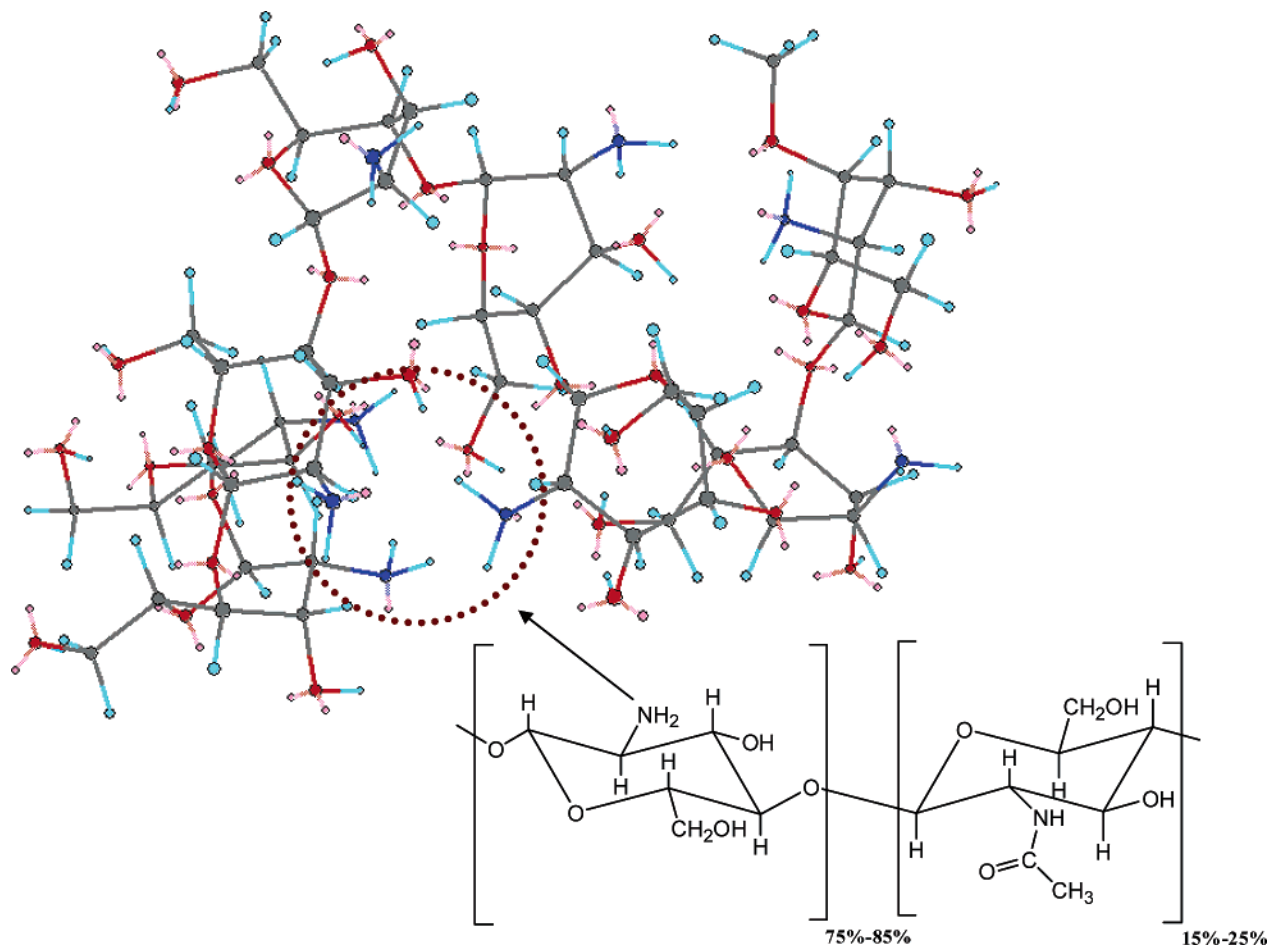


**Figure 1.** Schematic illustration of the composition and structure of the chitosan molecule. The conformation of the molecule was optimized by ChemBats3D through an energy-minimization program. Black, carbon; cyan, hydrogen; red, oxygen; navy, nitrogen. In this free state, the amine groups (highlighted with a dashed circle) are embedded in the random coils of the chitosan chains.

## Experimental Section

Chitosan with a molecular weight of 400 000 g/mol (75–85% deacetylated), tetrachloroauric(III) acid ( $\text{HAuCl}_4$ ), polycaprolactone (PCL), and rhodamine 6G were purchased from Aldrich-Sigma. PDMS elastomer kits (Sylgard 184) were obtained from Dow Corning (Midland, MI) to fabricate patterned surfaces molded from lithographically prepared masters, without any other treatment.<sup>16</sup> Chitosan was dissolved in 3% acetic acid (HAc) solution. Chitosan labeled with rhodamine B isothiocyanate (Aldrich) (Rd-chitosan) was prepared as follows: A 0.5% (w/v) chitosan solution was incubated with 2 mg/mL rhodamine B isothiocyanate at 4 °C for 48 h, and this solution was then dialyzed with 0.05 M acetic acid for 4 weeks.

To pattern the PDMS surface with chitosan, a glass slide, treated with piranha ( $\text{H}_2\text{SO}_4/\text{H}_2\text{O}$ , 70/30 v/v) solution, was immersed in a 0.4% chitosan/3% acetic acid solution for 12 h. Subsequently, the slide was pressed onto a flat or patterned PDMS film for 20 min to selectively transfer the chitosan molecules to the PDMS film or the ridges of the PDMS stamp.

Transmission electron microscopy (TEM) and electron diffraction were performed on a JEM-1200EX instrument (JEOL, Tokyo, Japan). As gold nanoparticles were tightly attached to the polymer surfaces, a thermal pressing method<sup>16b</sup> was used to transfer the particles onto PCL films in a viscoelastic state, and the PCL films were then consecutively cooled and dissolved with tetrahydrofuran (THF). After washing and exchange of THF with ethanol, the nanoparticles were supported on copper grids for TEM characterization. The sizes of the particles were determined by TEM.

Scanning electron microscopy (SEM) images were obtained on a SIRION instrument (FEI, Hillsboro, OR). Energy-dispersive spectroscopy (EDS) characterization was carried on a Phoenix EDAX system (GENESIS 4000) attached to the SEM, at the acceleration voltage of 10 keV. The signals were collected in the areas selected in the SEM images. A carbon layer instead of gold layer was electrodeposited on the samples before EDS characterization.

The surface morphology of samples was analyzed by topographic images collected by atomic force microscopy (AFM, SPI3800N, Seiko Instruments Inc., Chiba, Japan) in dynamic force mode. A silicon tip with a resonance frequency  $f_0$  of 150 kHz and a spring constant of 20 N/m was utilized. The scanning frequency was 0.5 Hz. The contact force between the tip and the samples was kept as low as possible (<2.5 nN).

Raman spectroscopy was performed under ambient conditions using a confocal Raman microscope (CRM200, WITec, Ulm, Germany) equipped with a piezo scanner (F-500, Physik Instrumente, Karlsruhe, Germany) and microscope objectives (20 $\times$ , NA = 0.40, Nikon). A circularly polarized laser (CrystaLaser,  $\lambda$  = 532 nm) was focused on the samples. The spectra were recorded at 1  $\text{cm}^{-1}$  resolution with 20-s accumulation times.

X-ray photoelectron spectroscopy (XPS) was conducted with an ESCA LAB Mark II spectrometer employing monochromatic X-ray Al K $\alpha$  excitation radiation ( $h\nu$  = 1486.6 eV, 150 W, 15 kV). The base pressure was  $2 \times 10^{-9}$  mbar. The charging shift was referred to the C(1s) line emitted from the saturated hydrocarbon. The take-off angle of the XPS was 90°. The constant-angle energy was 20 eV.

Fluorescence spectroscopy was performed on a Hitachi F-4500 fluorescence spectrophotometer. Rhodamine 6G was excited at 500 nm to produce the maximum emission of wavelengths at 540 nm. Fluorescence images were obtained by confocal laser scanning microscopy (CLSM, Bio-Rad Radiance 2100, Bio-Rad Laboratories,

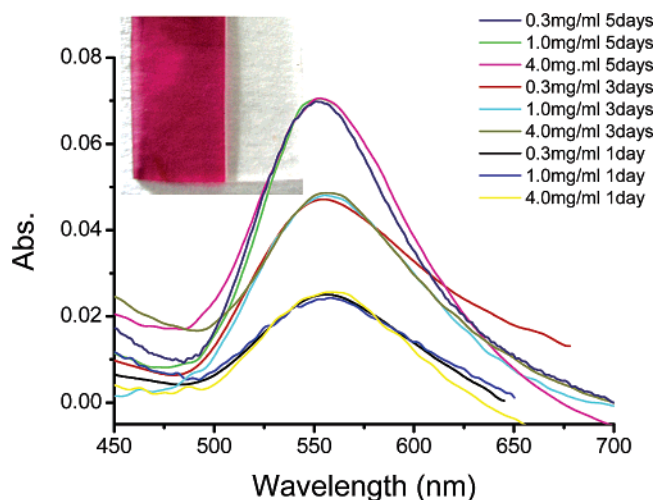


**Figure 2.** UV-vis spectra of PDMS films incubated in chitosan/HAc and HAuCl<sub>4</sub> aqueous solution, obtained using different chitosan concentrations and incubation times. Inset: Overall view of a PDMS film (right) and PDMS films covered with gold nanoparticles (left).

Hercules, CA). Specimens were excited at 543 nm. UV-vis spectra were recorded on a CARY 100 BIO spectrometer (Varian, Palo Alto, CA) in air. The absorbance of PDMS was used as the baseline. X-ray diffraction (XRD) patterns were obtained with a D/max-rA apparatus (Rigaku, Tokyo, Japan). Water contact angles were measured at room temperature using a DSA10-MK2 contact angle measuring system from Krüss. Prior to the measurements, all samples were dried at 30 °C under reduced pressure until a constant weight was reached, and the samples were stored in ambient air for 1 day.

Computation of scattering coefficients is based on Mie theory.<sup>17</sup> The calculations were performed with a home-built computer program based on MATLAB. A downward recurrence algorithm was utilized instead of the usual iteration. The set of dielectric data for gold was obtained from ref 18.

## Results and Discussion

Because of its low reducing ability, chitosan can be used as reducing agents/stabilizers to produce gold nanoparticles only at elevated temperature.<sup>12</sup> In the current work, we found that no gold nanoparticles formed when the mixture of HAuCl<sub>4</sub>/chitosan/HAc was stored at 4 °C for 6 months, as determined by UV-vis spectroscopy. In contrast, when a PDMS film was incubated in a mixture of chitosan and HAuCl<sub>4</sub> solutions, the film presented a reddish color within 2 h, while the solution phase remained yellow. Figure 2 shows the UV-vis spectra of the PDMS films obtained upon incubation in HAuCl<sub>4</sub>/chitosan solutions with different concentrations at 4 °C for different periods. The absorption bands centered at 548–550 nm are attributed to the surface plasmon band (SPB) of gold nanoparticles. The increase of extinction with reaction time reveals the formation and increasing population of gold nanoparticles. Both the intensity and the position of the SPB are independent of the concentrations of chitosan, HAc, and HAuCl<sub>4</sub>. The UV-vis spectra of the solutions showed no variation throughout the entire synthesis process, suggesting that no particles formed at 4 °C in solution. These results demonstrate that gold nanoparticles are selectively formed on the surfaces of the PDMS films.

Sharp diffraction peaks in the XRD patterns of the PDMS films obtained verify the formation of gold crystals on the film (Figure 3). A TEM image of the films (Figure 3, inset a) reveals that the shape of the gold nanocrystals is similar to that reported by Brust et al.<sup>19</sup> The gold nanoparticles obtained are quasi-

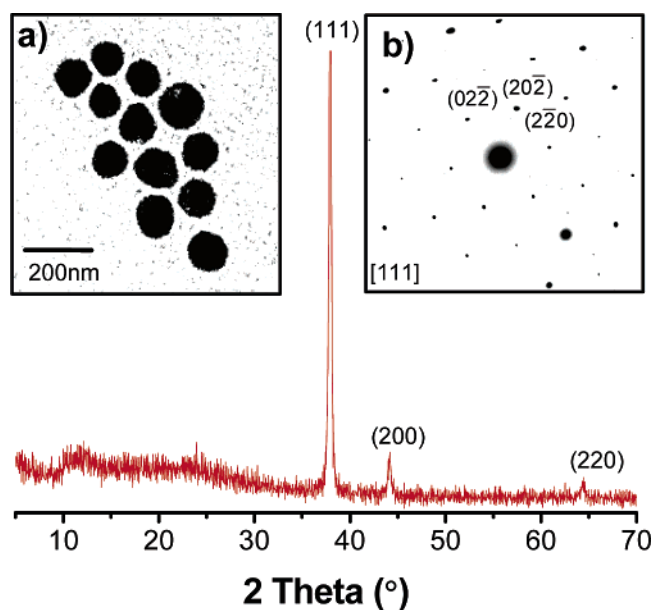


**Figure 3.** XRD pattern of gold nanoparticles formed on a PDMS film obtained upon incubation in chitosan/HAc and HAuCl<sub>4</sub> aqueous solution at 4 °C for 1 week. Insets: (a) Typical TEM image and (b) electron diffraction pattern of a single gold nanoparticle.

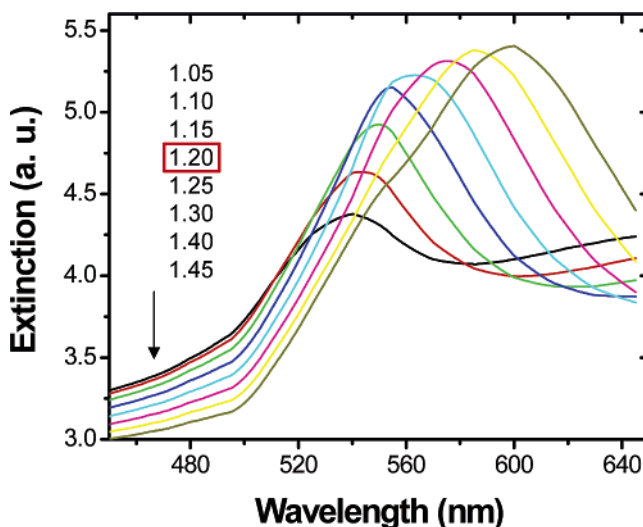


**Figure 4.** Calculated absorption spectra of colloidal gold particles with a diameter of 105 nm in media of different refractive indices. The red box indicates the value for which the calculated extinction is consistent with the experimental spectrum.

spherical and have a size of  $105 \pm 12$  nm. Electron diffraction confirms that the particles are single crystalline (Figure 3, inset b).

The nature of the SPB was rationalized by Mie in 1908.<sup>2c</sup> Mie theory attributes the SPB of spherical metallic particles to the dipole oscillation of the free electrons in the conduction band occupying the free energy states closely above the Fermi energy level, which can be described quantitatively by solving Maxwell's equations with appropriate boundary conditions.<sup>20</sup> The SPB maximum is sensitive to the size and shape of the particles, the temperature, and the dielectric constant of the medium.<sup>21</sup> Recently, the refractive index of the medium has been shown to induce a shift of the SPB in quantitative agreement with Mie theory.<sup>22</sup> Thus, the interpretation of UV-vis spectra can provide useful information about the medium surrounding the nanoparticles. Figure 4 displays the extinction spectra of gold nanoparticles with a diameter of 105 nm, as



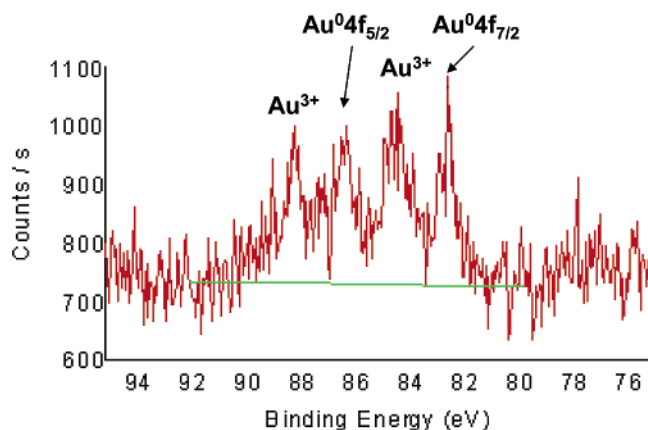


**Figure 5.** XPS spectrum of a PDMS surface after being incubated in chitosan/HAc and HAuCl<sub>4</sub> aqueous solution at 4 °C for 20 min.

calculated using different medium refractive indices. The SPB maximum shifts from 540 to 600 nm as the refractive index is increased from 1.05 to 1.45. Compared to the experimental spectra (Figure 2), the medium refractive index of the nanoparticles, obtained on the surface having an adsorbed chitosan layer, should be 1.20. Given that the refractive index of chitosan is 1.5<sup>23</sup> and that of air is around 1, the volume fraction of chitosan on the gold nanocrystals can be concluded to be 35%. This low coverage of chitosan on the gold nanoparticles suggests that the particles are attached onto the chitosan layer rather than being embedded inside. The independence of SPB and chitosan concentration implies that the major controlling factor is the adsorbed layer of chitosan, whose thickness is less dependent on the chitosan concentration than on the adsorption thermodynamics.

The formation of gold nanoparticles was confirmed by XPS characterization after the films had been incubated at 4 °C for 20 min (Figure 5). The binding energy of the doublet for Au 4f<sub>7/2</sub> and Au 4f<sub>5/2</sub> characteristic of Au<sup>0</sup> is clearly seen. The number and positions of the peaks are mostly consistent with the literature.<sup>24</sup> The shift of the Au(III) peaks can be attributed to the formation of Au–N electrostatic bonds.<sup>25</sup> Furthermore, the overlapping of the signal from Au(I), a transition state in the reduction process,<sup>26</sup> might also cause a shift in XPS.<sup>27</sup> This shows that Au<sup>0</sup> formed at the very early stage of reduction. It can be confirmed further that the ratio of Au<sup>0</sup> to Au(III) increased with prolonged time. The more important information provided by this experiment is that signals of Au(III) were also detected, revealing that gold ions were indeed attached to the surface via the chelating effect of the chitosan molecules.

Tetrachloroauric ions can form complexes with amine groups of chitosan on PDMS surfaces via electrostatic forces. The ions are subsequently reduced by the amine groups. After chitosan adsorption, the PDMS surface changed from hydrophobic to hydrophilic (ambient water contact angle  $\theta \approx 65^\circ$ ), which is significantly smaller than that of the cast chitosan film ( $\theta \approx 80^\circ$ ). This result reflects the occupation of different conformations by chitosan. As the amine groups of chitosan are more hydrophilic than the backbones, the adsorption of chitosan on the hydrophobic PDMS surface might yield more amine groups oriented toward the hydrophilic medium. In contrast, in the bulk solution, the amine groups could be embedded in the random coil of the chitosan molecules. The amine groups exposed on surfaces can act as the reducers/stabilizers that facilitate the formation of nanoparticles. In our synthesis process, oxidation of the amine groups by tetrachloroauric ions<sup>28</sup> occurred simultaneously with the formation of gold nanoparticles. Under these

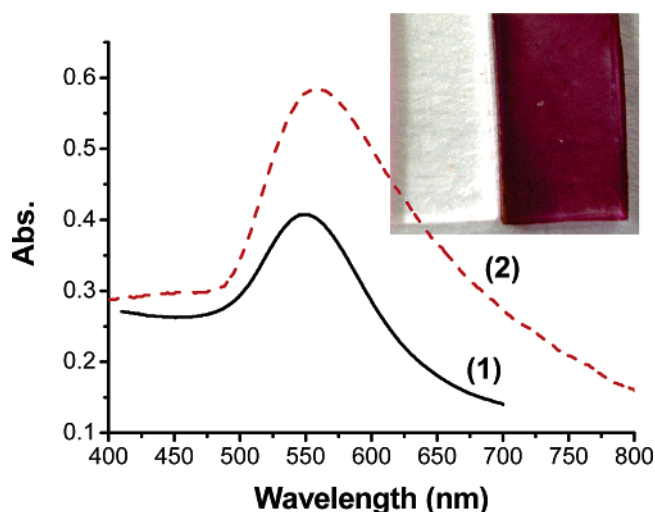


**Figure 6.** Surface plasmon absorption of PDMS films capped with (1) adsorbed and (2) printed chitosan layers after incubation in HAuCl<sub>4</sub> aqueous solution at 4 °C for 1 week. Inset: Overall view of a PDMS film (left) and PDMS films covered with gold nanoparticles formed on a printed chitosan layer (right).

mild conditions, not enough energy can be obtained by chloride ions in the bulk to form free radicals, resulting in the reduction of gold ions as in the case of photochemical synthesis.<sup>13b</sup> As a result, the gold nanoparticles were formed mainly on the chitosan layer rather than in the chitosan solution.

The two-dimensional growth of gold nanoparticles can also be used to explain why, in our work, the use of chitosan allows for the formation of nanoparticles at rather low temperature as compared to existing literature reports. The nucleation free energy is dramatically decreased on the interfaces by a factor of  $(2 + \cos \theta)(1 - \cos \theta)^2/4$ <sup>29</sup> (where  $\theta$  is the contact angle of the synthesis medium on the interface). Thus, the reduction reaction rate can be elevated exponentially on the polymer surface. The adsorption of chitosan molecules on the surface is sufficient for the formation of gold nanoparticles.

In this work, we also succeeded in growing gold nanoparticles on different polymer films, including polyester, polystyrene, and polyethylene. This demonstrates that the formation of gold nanoparticles is facilitated by the confinement of the surfaces and is independent of the chemical composition of the substrates.

Because only the chitosan layer adsorbed on the PDMS surface induced the formation of gold nanoparticles, we also accomplished the synthesis of gold nanoparticles by the micro-contact printing of chitosan molecules on the PDMS film. Printed with a flat glass slide as stamp, chitosan molecules were transferred from the glass surface to the PDMS surface. When the chitosan-printed PDMS films were immersed in HAuCl<sub>4</sub> solution for 1 week, the films became red (Figure 6, inset), slightly darker than the surfaces with adsorbed chitosan (Figure 2, inset). TEM indicated diameters of  $340 \pm 17$  nm for the gold particles formed on the printed chitosan layer after incubation in HAuCl<sub>4</sub> solution for 7 days, which is about 3 times larger than the particles formed on the adsorbed chitosan layer. The homogeneous appearance of the films demonstrates that the reaction is fairly uniform on the surfaces. Figure 6 shows that the resulting PDMS surface with a printed chitosan layer displayed a plasmon absorbance at 559–561 nm, exhibiting a red shift and broadening of the band as compared to chitosan-adsorbed substrates. This variation of extinction spectra has already been reported for silver nanoparticles with different sizes.<sup>30</sup> The amounts and conformations of the adsorbed and

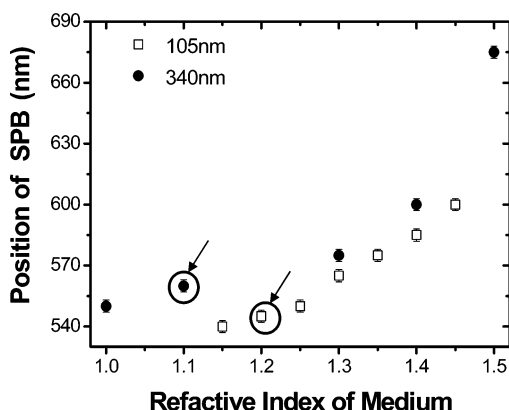


**Figure 7.** Plot of the SPB maxima of gold nanoparticles with diameters of 105 and 340 nm versus the refractive index of the medium. The arrows indicate the experimental values.

printed chitosan molecules are both different,<sup>16b,31</sup> which will affect the size of the produced particles.<sup>12a</sup>

As shown in Figure 7, the medium refractive index of the gold nanoparticles produced on the printed chitosan layer is 1.10, corresponding to a degree of coverage of  $\sim 17\%$  chitosan molecules on the gold nanoparticles. This calculation indicates that it is difficult for the particles to penetrate into and be embedded in the printed chitosan layer, as the printed layer is expected to be much more densely packed than the adsorbed layer.<sup>31a</sup> In our previous study, quantitative measurements indicated that the density of a printed layer can be 10–20 times that of an adsorbed layer, depending on the nature of the biomacromolecules.<sup>31a</sup>

When PDMS substrates with topologically circular patterns were used, chitosan tended to accumulate at the boundary of the topographical inflection, e.g., the boundary of the patterns,<sup>16b</sup> as a result of capillary forces.<sup>32</sup> Our previous study<sup>16b</sup> suggested that the adsorption of molecules on structured surfaces is a kinetics-controlled process in which the shapes of the patterns obtained depend on the adsorption time. Visualized by the fluorescence of Rd-chitosan, ring-shaped patterns were observed on the topologically patterned PDMS surfaces, obtained after a 20-min adsorption time (Figure 8a). After incubation in  $\text{HAuCl}_4$  solution, gold nanoparticles were selectively formed within the chitosan-loaded rings (Figure 8b). Fluorescence spectra (Figure 9) show that the fluorescence of rhodamine is completely quenched by the gold nanoparticles, as a result of energy transfer from the excited fluorophores to the particles, leading to an enhancement in the energy-transfer efficiency.<sup>33</sup> Furthermore, the strong absorption and local maximum characteristic of SPB of the gold nanoparticles on the PDMS surface provide an additional decay channel for nonradiative energy transfer.<sup>34</sup>

The metal-cluster-induced quenching of fluorescent probes has been utilized in the analysis of trace molecules, such as DNA, with higher sensitivity than any other probes currently available.<sup>34</sup> A similar phenomenon was also demonstrated previously on charged colloids.<sup>35</sup> On the other hand, surface plasmon excitation can dramatically increase the electromagnetic field near particle surfaces, resulting in surface-enhanced Raman scattering (SERS).<sup>36</sup>

In this work, the gold nanoparticles obtained on the chitosan layers on the PDMS substrates were rather loosely coated by the chitosan chains, so their surfaces might be expected to be directly exposed to the surroundings, allowing for the adsorption of different molecules in the medium. It has been reported that most fluorescent dyes spontaneously adsorb on gold and silver surfaces.<sup>37</sup> In fact, the binding equilibrium constant between

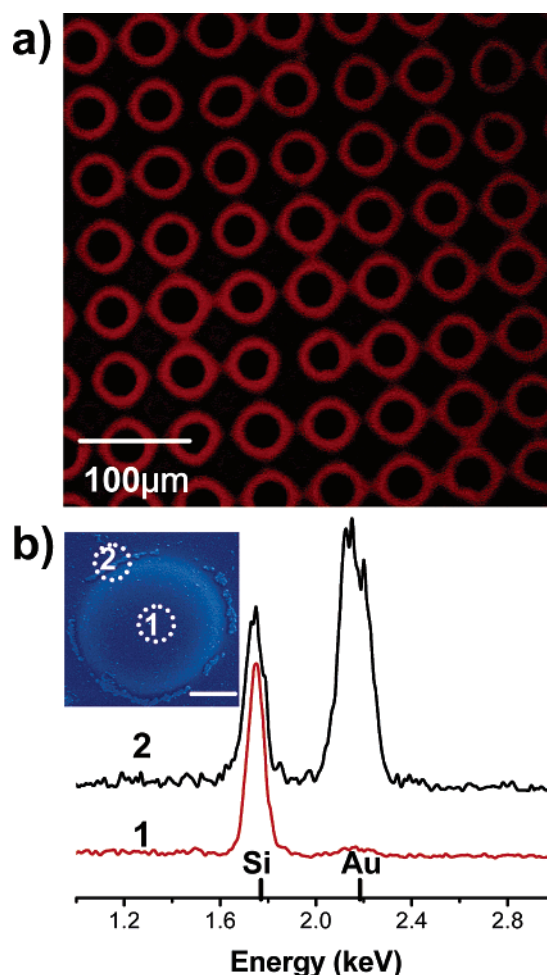


**Figure 8.** (a) CLSM image of the Rd-chitosan patterns formed on a microstructured PDMS surface by incubating the film in 0.4% Rd-chitosan aqueous solution for 20 min. The topological patterns on the surface are arrays of columns with a diameter of  $45 \mu\text{m}$  and a spacing of  $15 \mu\text{m}$ . (b) EDS spectra collected from (1) chitosan-uncapped and (2) chitosan-capped regions shown in the inset. Inset: SEM image of the gold nanoparticle patterns on a chitosan-patterned PDMS film formed after incubation in  $\text{HAuCl}_4$  solution for 1 week. The scale bar is  $10 \mu\text{m}$ .

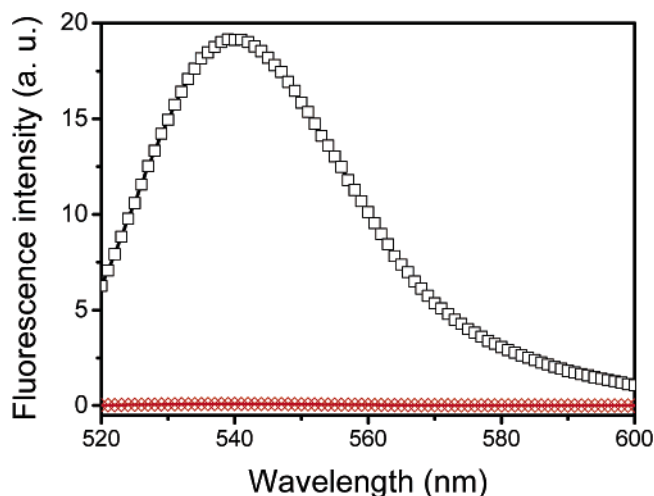


**Figure 9.** Fluorescence spectra of Rd-chitosan-capped PDMS films before (upper line) and after (bottom line) incubation in  $\text{HAuCl}_4$  aqueous solution for 7 days.

rhodamine 6G and silver is approximately  $10^9$ .<sup>38</sup> The proximity ( $< 10 \text{ nm}$ ) of a fluorophore to the gold surface guarantees the

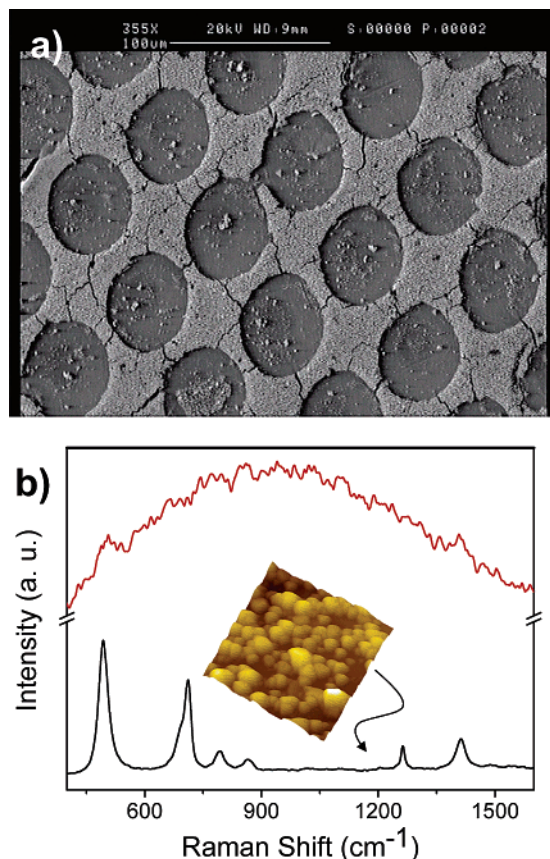


**Figure 10.** (a) SEM image of gold nanoparticle patterns on a chitosan-patterned PDMS film with microwells of 50  $\mu\text{m}$  and a spacing of 10  $\mu\text{m}$ . Continuous regions are protruding and were precovered with chitosan via printing. (b) Raman spectra of the regions uncapped (upper line) and capped (bottom line) by gold nanoparticles on the surfaces shown in a after they had been dipped in 10  $\mu\text{g/mL}$  rhodamine 6G solution. Two measurements were made using identical conditions. The Raman bands at 490, 708, 793, 863, 1260, and 1401  $\text{cm}^{-1}$  can be assigned to the Si–O symmetric stretch, C–Si–C symmetric stretch, C–Si–C asymmetric stretch,  $\text{CH}_3$  rock, C–H symmetric bend, and C–H symmetric bend, respectively.<sup>40</sup> Inset: Magnified AFM image showing the topology of the gold-nanoparticle-capped regions. The scanning area is 5  $\mu\text{m} \times 5 \mu\text{m}$ .

strong quenching of rhodamine.<sup>39</sup> Therefore, we used the gold nanoparticles to detect trace quantities of analytes on the basis of quenching and the SERS effect.

As we reported before, chitosan can be easily contact-printed onto the protruding parts of patterned surfaces.<sup>16b</sup> When such a chitosan-patterned surface (exemplified with arrays of microwells) was immersed in  $\text{HAuCl}_4$  aqueous solution, patterns of gold particles with high selectivity could be formed within 1 week (Figure 10a). The most remarkable feature is the high density of gold particles in the protruding areas covered with chitosan.

These patterned films were dipped in 10  $\mu\text{g/mL}$  rhodamine 6G solution for 20 min and then observed by confocal Raman spectroscopy. The regions not capped with gold nanoparticles showed strong fluorescence of rhodamine 6G, which made Raman bands unobservable (Figure 10b, upper line). By contrast, in the gold-nanoparticle-capped regions, the strong fluorescence was quenched by the nanoparticles, and the Raman bands were sharp and clear (Figure 10b, lower line). All of these results suggest that the fluorescence can be quenched, allowing Raman signals to be detected on the surfaces with spatial selectivity. The absence of the SERS effect of the chitosan layer can be attributed to two effects. First, the Raman bands of PDMS are

much stronger than and also overlap those of chitosan molecules. Second, the chitosan layer was too thin (the thickness was no more than 5 nm) to be focused for detection of their weak signals.

## Conclusions

We successfully demonstrate a facile method for synthesizing gold nanoparticles by the incubation of chitosan-capped PDMS films in  $\text{HAuCl}_4$  solution. Exploiting 2D surface confinement, we demonstrated that the formation of gold nanoparticles can be accomplished at room temperature and 4  $^\circ\text{C}$ , which is substantially different from previous literature reports. Only the chitosan molecules on the surfaces play a role in synthesis. Chitosan layers printed and adsorbed on surfaces resulted in gold nanoparticles with different sizes. Computation of the SPB suggests a rather low degree of coverage of chitosan molecules on the nanoparticles. Colloidal gold nanoparticles were further fabricated on chitosan-patterned PDMS surfaces, showing quenching effect of fluorophores and enhanced Raman scattering. The combination of SERS and regional quenching should be of great importance for observations of the diffusion of molecules and the mobility of cells.

**Acknowledgment.** Y. Y. Chen, J. C. Shen, D. J. Xu, and Y. W. Wang are appreciated for their stimulating discussions. We also thank J. Wang and D. P. Chen at USTC for XPS measurements. B.W. and W.J.T. thank the Max-Planck Society and Prof. H. Möhwald for visiting scientist grants. This study was financially supported by the National Science Fund for Distinguished Young Scholars of China (No. 50425311), the Major State Basic Research Program of China (2005CB623902), and the Natural Science Foundation of China (No. 20434030).

## References and Notes

- (1) (a) Murray, C. B.; Norris, D. J.; Bawendi, M. G. *J. Am. Chem. Soc.* **1993**, *115*, 8706. (b) Ahmadi, T. S.; Wang, Z. L.; Green, T. C.; Henglein, A.; El-sayed, M. A. *Science* **1996**, *272*, 1924. (c) Teranishi, T.; Hosoe, M.; Miyake, M. *Adv. Mater.* **1997**, *9*, 65. (d) Sun, S. H.; Murray, C. B.; Weller, D.; Folks, L.; Moser, A. *Science* **2000**, *287*, 1989. (e) Puentes, V. F.; Krishnan, K. M.; Alivisatos, A. P. *Science* **2001**, *291*, 2115. (f) Stoeva, S.; Klabunde, K. J.; Sorensen, C. M.; Dragieva, I. *J. Am. Chem. Soc.* **2002**, *124*, 2305. (g) Hassenkam, T.; Nørsgaard, K.; Iversen, L.; Kiely, C.; Brust, M.; Bjørnholm, T. *Adv. Mater.* **2002**, *14*, 1126. (h) Penner, R. M. *J. Phys. Chem. B* **2002**, *106*, 3339. (i) Sun, X.; Dong, S.; Wang, E. *Angew. Chem., Int. Ed.* **2004**, *43*, 6360.
- (2) (a) Cao, Y. W. C.; Jin, R.; Mirkin, C. A. *Science* **2002**, *297*, 1536. (b) Mohr, C.; Hofmeister, H.; Radnik, J.; Claus, P. *J. Am. Chem. Soc.* **2003**, *125*, 1905. (c) Daniel, M.; Astruc, D. *Chem. Rev.* **2004**, *104*, 293. (d) Katz, E.; Willner, I. *Angew. Chem., Int. Ed.* **2004**, *43*, 6042. (e) Kato, N.; Caruso, F. *J. Phys. Chem. B* **2005**, *109*, 19604.
- (3) (a) Turkevitch, J.; Stevenson, P. C.; Hillier, J. *Discuss. Faraday Soc.* **1951**, *11*, 55. (b) Brust, M.; Walker, M.; Bethell, D.; Schiffrin, D. J.; Whyman, R. *J. Chem. Soc., Chem. Commun.* **1994**, 801.
- (4) Yee, C.; Scotti, M.; Ulman, A.; White, H.; Rafailovich, M.; Sokolov, J. *Langmuir* **1999**, *15*, 4314.
- (5) (a) Kerker, M. *J. Colloid Interface Sci.* **1986**, *112*, 302. (b) Toshima, N.; Yonezawa, T. *New J. Chem.* **1998**, *22*, 1179.
- (6) Turkevitch, J.; Steven, P. C.; Hiller, J. *Discuss. Faraday Soc.* **1951**, *11*, 55.
- (7) Hirai, H.; Chawanya, H.; Toshima, N. *React. Polym.* **1985**, *3*, 127.
- (8) (a) Mucic, R. C.; Storhoff, J. J.; Mirkin, C. A.; Letsinger, R. L. *J. Am. Chem. Soc.* **1998**, *120*, 12674. (b) Raveendran, P.; Fu, J.; Wallen, S. L. *J. Am. Chem. Soc.* **2003**, *125*, 13940.
- (9) Mukherjee, P.; Ahmad, A.; Mandal, D.; Senapati, S.; Sainkar, S. R.; Khan, M. I.; Parishcha, R.; Ajaykumar, P. V.; Alam, M.; Kumar, R.; Sastry, M. *Nano Lett.* **2001**, *1* (10), 515. (b) Mukherjee, P.; Ahmad, A.; Mandal, D.; Senapati, S.; Sainkar, S. R.; Khan, M. I.; Ramani, R.; Parishcha, R.; Ajaykumar, P. V.; Alam, M.; Sastry, M.; Kumar, R. *Angew. Chem., Int. Ed.* **2001**, *40*, 3585.



- (10) Wu, L. Q.; Lee, K.; Wang, X.; English, D. S.; Losert, W.; Payne, G. F. *Langmuir* **2005**, *21*, 3641.
- (11) Yonezawa, Y.; Kawabata, I.; Sato, T. *Ber. Bunsen-Ges. Phys. Chem.* **1996**, *100*, 39.
- (12) (a) Esumi, K.; Takei, N.; Yoshimura, T. *Colloids Surf. B: Biointerfaces* **2003**, *32*, 117. (b) Huang, H.; Yang, X. *Biomacromolecules* **2004**, *5*, 2340. (c) dos Santos, D. S., Jr.; Goulet, P. J. G.; Pieczonka, N. P. W.; Oliveira, O. N., Jr.; Aroca, R. F. *Langmuir* **2004**, *20*, 10273.
- (13) (a) Miyama, T.; Yonezawa, Y.; Sato, T.; Kawabata, I. *Chem. Lett.* **1994**, 355. (b) Miyama, T.; Yonezawa, Y. *Langmuir* **2004**, *20*, 5918.
- (14) Ishizuki, N.; Torigoe, K.; Esumi, K.; Meguro, K. *Colloids Surf.* **1991**, *55*, 15.
- (15) (a) Ly Arrascue, M.; Maldonado, Garcia, H.; Horna, O.; Guibal, E. *Hydrometallurgy* **2003**, *71*, 191. (b) Guibal, E. *Prog. Polym. Sci.* **2005**, *30*, 71.
- (16) (a) Xia, Y.; Whitesides, G. M. *Angew. Chem., Int. Ed.* **1998**, *37*, 550. (b) Wang, B.; Feng, J.; Gao, C. *Chem. Mater.* **2004**, *16*, 4859.
- (17) Bohren, C. F.; Huffman, D. R. *Absorption and Scattering of Light by Small Particles*; Wiley: New York, 1983.
- (18) (a) Johnson, P. B.; Christy, R. W. *Phys. Rev. B* **1972**, *8*, 4370. (b) Ordal, M. A.; Long, L. L.; Bell, R. J.; Bell, S. E.; Alexander, R. W., Jr.; Ward, C. A. *Appl. Opt.* **1983**, *22*, 1099.
- (19) Brust, M.; Fink, J.; Bethell, D.; Schiffrin, D. J.; Kiely, C. J. *J. Chem. Soc., Chem. Commun.* **1995**, 1655.
- (20) Alvarez, M. M.; Khoury, J. T.; Schaaff, T. G.; Shafigullin, M. N.; Vezmar, I.; Whetten, R. L. *J. Phys. Chem. B* **1997**, *101*, 3706.
- (21) (a) Ishizuki, N.; Torigoe, K.; Esumi, K.; Meguro, K. *Colloids Surf.* **1991**, *55*, 15. (b) Patton, D.; Locklin, J.; Meredith, M.; Xin, Y.; Advincula, R. *Chem. Mater.* **2004**, *16*, 5063.
- (22) (a) Underwood, S.; Mulvaney, P. *Langmuir* **1994**, *10*, 3427. (b) Mulvaney, P. *Langmuir* **1996**, *12*, 788.
- (23) Jiang, H.; Su, W.; Caracci, S.; Bruning, T. J.; Cooper, T.; Adams, W. *J. Appl. Polym. Sci.* **1996**, *61*, 1163.
- (24) (a) Boyen, H. G.; Kästle, G. *Science* **2002**, *297*, 1533. (b) Jaramillo, T. F.; Baeck, S.; Cuenya, B. R.; McFarland, E. W. *J. Am. Chem. Soc.* **2003**, *125*, 7148.
- (25) Remita, H.; Etcheberry, A.; Belloni, J. *J. Phys. Chem. B* **2003**, *107*, 31.
- (26) Gachard, E.; Remita, H.; Khatouri, J.; Keita, B.; Nadjio, L.; Belloni, J. *New J. Chem.* **1998**, 1257.
- (27) Stoycheva-Topalova, R.; Assa, J.; Buroff, A.; Tzvetkov, T.; Necheva, S.; Drandarov, N.; Vichev, R.; Blanpain, B. *Vacuum* **1998**, *51*, 273.
- (28) Kinyanjui, J. M.; Hatchett, D. W.; Smith, J. A.; Josowicz, M. *Chem. Mater.* **2004**, *16*, 3390.
- (29) Grosso, G.; Parravicini, G. P. *Solid-State Physics*; Academic Press: San Diego, 2000.
- (30) (a) Kim, H. S.; Ryu, J. H.; Jose, B.; Lee, B. G.; Ahn, B. S.; Kang, Y. S. *Langmuir* **2001**, *105*, 8785. (b) Zhang, J.; Malicka J.; Gryczynski, I.; Lakowicz, J. R. *J. Phys. Chem. B* **2005**, *109*, 7643.
- (31) (a) Wang, B.; Feng, J.; Gao, C. *Macromol. Biosci.* **2005**, *5*, 767. (b) Biasco, A.; Pisignano, D.; Krebs, B.; Pompa, P. P.; Persano, L.; Cingolani, R.; Rinaldi, R. *Langmuir* **2005**, *21*, 5154.
- (32) Xia, Y.; Qin, D.; Yin, Y. *Curr. Opin. Colloid Interface Sci.* **2001**, *6*, 54.
- (33) Maxwell, D. J.; Taylor, J. R.; Nie, S. *J. Am. Chem. Soc.* **2002**, *124*, 9606.
- (34) Dubertret, B.; Calame, M.; Libchaber, A. *Nat. Biotechnol.* **2001**, *19*, 365.
- (35) Jeon, S.; Granick, S. *Colloid Surf. A: Physicochem. Eng. Aspects* **2004**, *238*, 109.
- (36) (a) Sokolov, K.; Chumanov, G.; Cotton, T. M. *Anal. Chem.* **1998**, *70*, 3898. (b) Miyama, T.; Yonezawa, Y.; Sato, T.; Umemura, J.; Takenaka, T. *Chem. Lett.* **1993**, 1537.
- (37) Nie, S. M.; Emory, S. R. *Science* **1997**, *275*, 1102.
- (38) Hildebrandt, P.; Stockburger, M. *J. Phys. Chem.* **1984**, *88*, 5935.
- (39) Pérez-Luna, V. H.; Yang, S.; Rabinovich, E. M.; Buranda, T.; Sklar, L. A.; Hampton, P. D.; López, G. P. *Biosens. Bioelectron.* **2002**, *17*, 71.
- (40) Jayes, L.; Hard, A. P.; Séné, C.; Parker, S. F.; Jayasooriya, U. A. *Anal. Chem.* **2003**, *75*, 742.

BM060030F